



# Molecular tools that block maturation of the nuclear lamin A and decelerate cancer cell migration

Alexios N. Matralis<sup>a,1</sup>, Dimitrios Xanthopoulos<sup>a</sup>, Geneviève Huot<sup>b</sup>, Stéphane Lopes-Paciencia<sup>b</sup>, Charles Cole<sup>a,1</sup>, Hugo de Vries<sup>a,1</sup>, Gerardo Ferbeyre<sup>b</sup>, Youla S. Tsantrizos<sup>a,c,\*</sup>

<sup>a</sup> Department of Chemistry, McGill University, 801 Sherbrooke Street West, Montreal, QC H3A 0B8, Canada

<sup>b</sup> Département de Biochimie et médecine moléculaire, CRCHUM, Université de Montréal, C.P. 6128, Succ. Centre-Ville, Montréal, Québec H3C 3J7, Canada

<sup>c</sup> Department of Biochemistry, McGill University, 3649 Promenade Sir William Osler, Montreal, QC H3G 0B1, Canada

## ARTICLE INFO

### Keywords:

Prelamin A  
Zinc metalloprotease STE24  
ZPMSTE24  
Lamin A

## ABSTRACT

Lamin A contributes to the structure of nuclei in all mammalian cells and plays an important role in cell division and migration. Mature lamin A is derived from a farnesylated precursor protein, known as prelamins A, which undergoes post-translational cleavage catalyzed by the zinc metalloprotease STE24 (ZPMSTE24). Accumulation of farnesylated prelamins A in the nuclear envelope compromises cell division, impairs mitosis and induces an increased expression of inflammatory gene products. ZPMSTE24 has been proposed as a potential therapeutic target in oncology. A library of peptidomimetic compounds were synthesized and screened for their ability to induce accumulation of prelamins A in cancer cells and block cell migration in pancreatic ductal adenocarcinoma cells. The results of this study suggest that inhibitors of lamin A maturation may interfere with cell migration, the biological process required for cancer metastasis.

## 1. Introduction

The nuclear lamina is composed of several lamin-type proteins that include lamin A as a key component. Lamin A is derived from a precursor protein, known as prelamins A, which undergoes four post-translational modifications before releasing the mature lamin A (Fig. 1).<sup>1</sup> First prelamins A is farnesylated at the C-terminal cysteine residue of the CaaX motif (Fig. 1; intermediate I); a modification which contributes to its localization at the nuclear membrane. Second, the three C-terminal amino acids (*i.e.* -aaX) are cleaved-off by the human zinc metalloprotease STE24 (ZPMSTE24; also known as FACE1) leading to intermediate II. However, a biochemical redundancy mechanism exists for this second step that can allow alternative processing of intermediate I to II by the Ras converting endopeptidase 1 (RCE1). Third, the farnesylcysteine residue of intermediate II is converted to the methyl ester intermediate III, under the catalytic activity of isoprenylcysteine carboxyl methyltransferase (ICMT). Finally, the last 15 amino acids (containing the farnesylated cysteine residue) are cleaved-off by ZPMSTE24, releasing the mature lamin A protein. Currently, ZPMSTE24 is the only known enzyme that can perform this last critical endoproteolytic cleavage and prelamins A is the only known mammalian substrate of this enzyme. Therefore, ZPMSTE24 plays a key role in the

maturation of the nuclear envelope filament lamin A, contributing to the structure of nuclei in all mammalian cells.<sup>2</sup> Inhibition of ZPMSTE24 leads to accumulation of the farnesylated prelamins A and premature cell senescence. Unlike apoptosis, cellular senescence is a permanent cell cycle arrest that halts tumorigenesis and simultaneously activates antitumor immune responses.<sup>3</sup> Consequently, it has been proposed that inhibitors of ZPMSTE24 may act as senescence agonists.<sup>4</sup>

Hutchinson-Gilford Progeria Syndrome (HGPS) is a rare genetic disease, which mimics some aspects of human aging.<sup>5</sup> HGPS cells accumulate a variant of prelamins A, known as progerin, which cannot be cleaved by ZPMSTE24 and presumed to be responsible for the disease symptoms. Cells expressing progerin have genomic instability,<sup>6</sup> telomere dysfunction,<sup>7</sup> altered epigenetic modifications of histones,<sup>8</sup> abnormal chromosome segregation, binucleation<sup>9</sup> and changes in nuclear architecture.<sup>10</sup> However, the exact molecular mechanism(s) explaining all these alterations and their connection to cellular senescence is still unknown. Therapeutic agents that block the biosynthesis of farnesylated prelamins A in cells provide some *in vivo* benefits, both in humans and animal models of HGPS. For example, a combination treatment with pravastatin (1) and zoledronic acid (2), was found to extend longevity in a mouse model of human premature aging (Fig. 2).<sup>11</sup> Pravastatin (1) and zoledronic acid (2), are clinically validated drugs

\* Corresponding author at: Department of Chemistry, McGill University, 801 Sherbrooke Street West, Montreal, QC H3A 0B8, Canada.  
E-mail address: [Youla.tsantrizos@mcgill.ca](mailto:Youla.tsantrizos@mcgill.ca) (Y.S. Tsantrizos).

<sup>1</sup> Current address: Alexander Fleming Biomedical Sciences Research Center, Division of Immunology, Athens 16672, Greece.

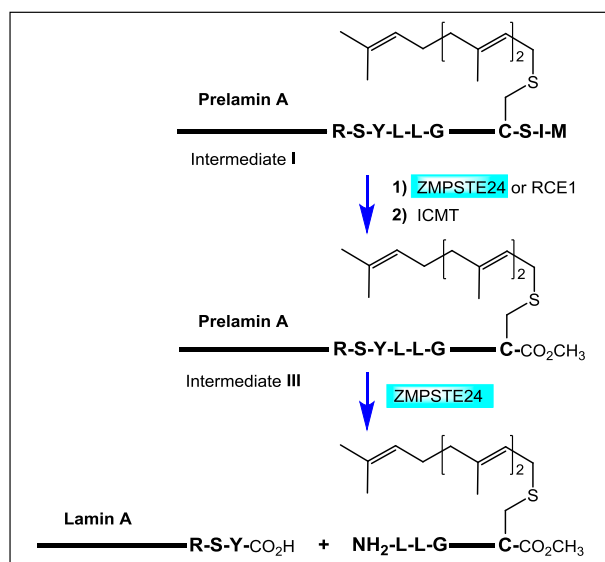


**Figure 1.** Biogenesis of mature lamin A from prelamins; key enzymes involved in the last three steps of the post-translational modifications of prelamins A are indicated, particularly the role of the zinc metalloprotease STE24 (ZMPSTE24), which is highlighted in blue. (For interpretation of the references to color in this figure legend, the reader is referred to the web version of this article.)

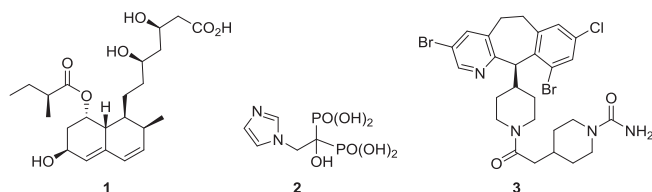


**Figure 2.** Inhibitors of isoprenoid biosynthesis and/or protein prenylation; pravastatin (1), zoledronic acid (2), and lonafarnib (3) inhibiting HMG-CoA reductase, farnesyl pyrophosphate synthase (hFPPS), farnesyl transferase enzyme (FTPase), respectively.

that specifically target the mevalonate pathway, inhibiting HMG-CoA reductase and farnesyl pyrophosphate synthase (hFPPS), respectively. These drugs block isoprenoid biosynthesis and consequently, farnesylation of prelamins A. Similarly, inhibition of the farnesyl transferase enzyme (FTPase) with lonafarnib (3) in monotherapy,<sup>12</sup> or in combination with 1 and 2 have been shown to ameliorate some aspects of the cardiovascular and bone diseases afflicting children with HGPS.<sup>13</sup> Interestingly, cancers are extremely rare in children with HGPS, despite their accelerated aging and the typically expected increase in cancer rates as a consequence of aging.<sup>14</sup> A possible explanation for this observation could be that children with HGPS do not live long enough to provide statistically reliable epidemiology. Alternatively, it has been proposed that the accumulation of prenylated prelamins A may lead to impaired cell cycle progression that halts cancer progression in these children. In support of this hypothesis, genetically engineered *Zmpste24* knockout mice were shown to be resistant to cancer invasion.<sup>15</sup> Collectively, all recent biochemical findings suggest that inhibition of ZMPSTE24 will block maturation of lamin A and induce cell senescence, providing a novel mechanism for the treatment of cancer. However, in the absence of potent and selective inhibitors of ZMPSTE24, validation of this enzyme as a therapeutic target remains a speculation.

Over the last few years, we have been investigating the association between age-related diseases and isoprenoid metabolism in mammals, including humans. For example, we recently showed that down-regulation of the intracellular levels of farnesyl pyrophosphate (FPP) and geranylgeranyl pyrophosphate (GGPP) can be therapeutically

useful mechanisms for the treatment of some age-related cancers (e.g. multiple myeloma)<sup>16</sup> and tau-related pathologies, such as the Alzheimer's disease.<sup>17</sup> In this study, we report the design of a new class of compounds that induce intracellular accumulation of farnesylated prelamins A in human cancer cells, including osteosarcoma (U-2 OS), pancreatic adenocarcinoma (HPAF-II, SW1990, KP-4) and colon carcinoma (HCT-116). Furthermore, a phosphinyl derivative was identified, which not only induces accumulation of prelamins A in one of the most highly tumorigenic pancreatic cancer cell lines (KP-4), but it also decreases the transmigration potential of these cells, without inducing any significant toxicity to either the KP-4 cells or normal fibroblasts (IMR-90). Optimization of this class of compounds could plausibly lead to the identification of novel antitumor agents that can block both cancer cells proliferation and migration/metastasis.

## 2. Results and discussion

To date, selective inhibitors of ZMPSTE24 have not been identified. Structural information that could potentially guide the design of inhibitors for this target is also limited to only two structures of the human recombinant enzyme<sup>2,18</sup> and one of the *S. cerevisiae*<sup>19</sup> enzyme. Unfortunately, these structures provide insufficient information about the molecular recognition elements that dictate binding of ligands to the active site of ZMPSTE24 (i.e. high resolution data at the atomic level of ZMPSTE24/ligand co-crystal structures). Consequently, these structures cannot effectively guide structure-based drug design. Identification of hits via high throughput screening (HTS) has not been reported for this target; it is anticipated that such efforts would be very challenging due to the biophysical nature of this protein. ZMPSTE24 is a highly membrane-bound enzyme that adopts a seven transmembrane  $\alpha$ -helical barrel structure,<sup>2,18</sup> thus requiring high concentrations of detergents and/or protein-lipid micelle-bound protein preparations in order to be rendered soluble. Such conditions are not ideal for HTS nor structure-activity relationship (SAR) studies, as *in vitro* testing would be highly prone to false positive/negative results. To date, biochemical studies on the inhibition of ZMPSTE24 have been conducted primarily using indirect inhibition assays, most often coupled to the methylation step catalyzed by ICMT, rather than direct *in vitro* assays of a soluble form of the human recombinant ZMPSTE24. Therefore, the binding affinity of any ligand for this target and the details on its interactions with ZMPSTE24 remain unclear.

HIV protease inhibitors (HIV PIs), such as lopinavir (4), ritonavir (5)<sup>18,20</sup> and atazanavir (6),<sup>18,21</sup> have been reported to weakly inhibit ZMPSTE24, leading to the accumulation of prelamins A in cellular assays (Fig. 3, compounds 4–6). It is noteworthy that clinical observations from HIV infected patients treated with these drugs are inconsistent or contradictory to these findings.<sup>22</sup> However, this discrepancy may be due to the low affinity of these compounds for ZMPSTE24, their high protein binding and the differences between protein concentrations in cultured cells *versus* human plasma. Inhibition of ZMPSTE24 with the only non-peptidic HIV PI, tipranavir<sup>18</sup> and accumulation of prelamins A in human fibroblasts treated with geranylgeranyl transferase I (GGTase I) inhibitors have also been reported.<sup>23</sup> However, the structural features of these latter compounds deviate significantly from those of the peptidomimetics 4–6.

We initiated our medicinal chemistry efforts with the knowledge that aspartate proteases (e.g. HIV protease) and the zinc metalloproteases (e.g. ZMPSTE24, thermolysin, angiotensin converting enzyme and others) share a common mechanistic action. Both families of enzymes use a water molecule as the nucleophile that attacks the scissile amide bond. This is in contrast to the serine/cysteine proteases, which use the side chain of a nucleophilic amino acid residue to initiate amide bond hydrolysis. Based on the mechanistic similarities of aspartate proteases and the zinc metalloprotease, we designed a minimal consensus scaffold of well-known inhibitors of such enzymes (Fig. 3). A common structural motif of the peptidomimetic HIV PIs is the central

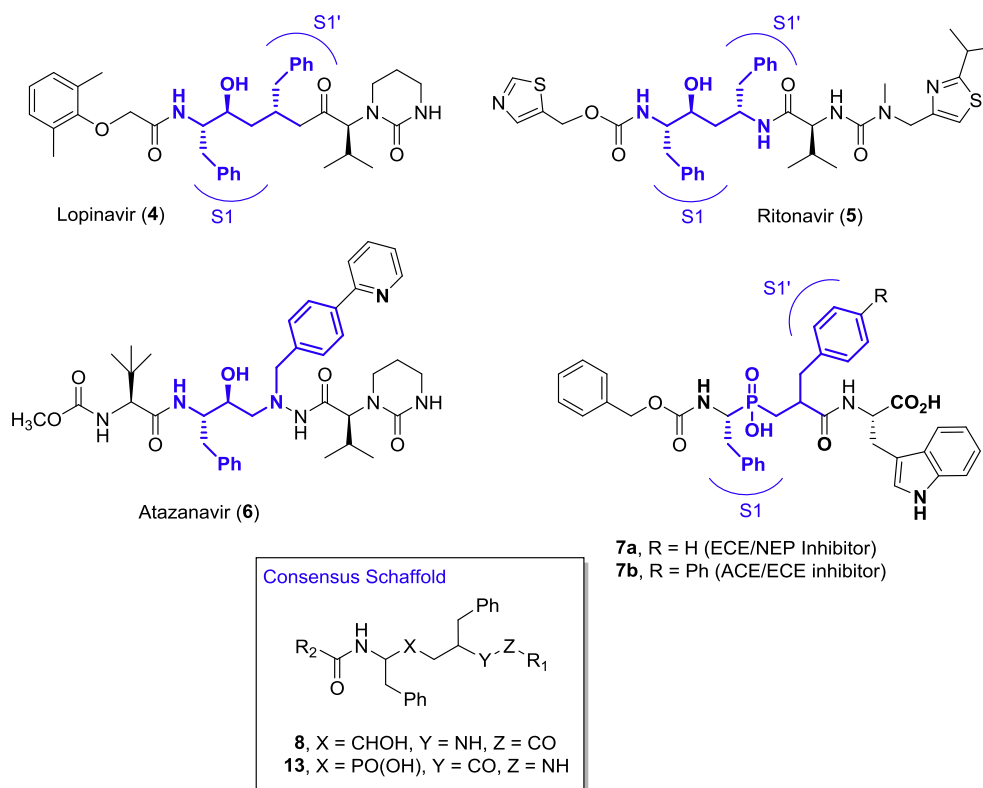


**Figure 3.** Structures of previously known ZMPSTE24 inhibitors. The key transition-state mimics, the hydroxyethylene moiety of 4 and 5, and the phosphinic acid moiety of 7 are highlighted in blue color. (For interpretation of the references to color in this figure legend, the reader is referred to the web version of this article.)

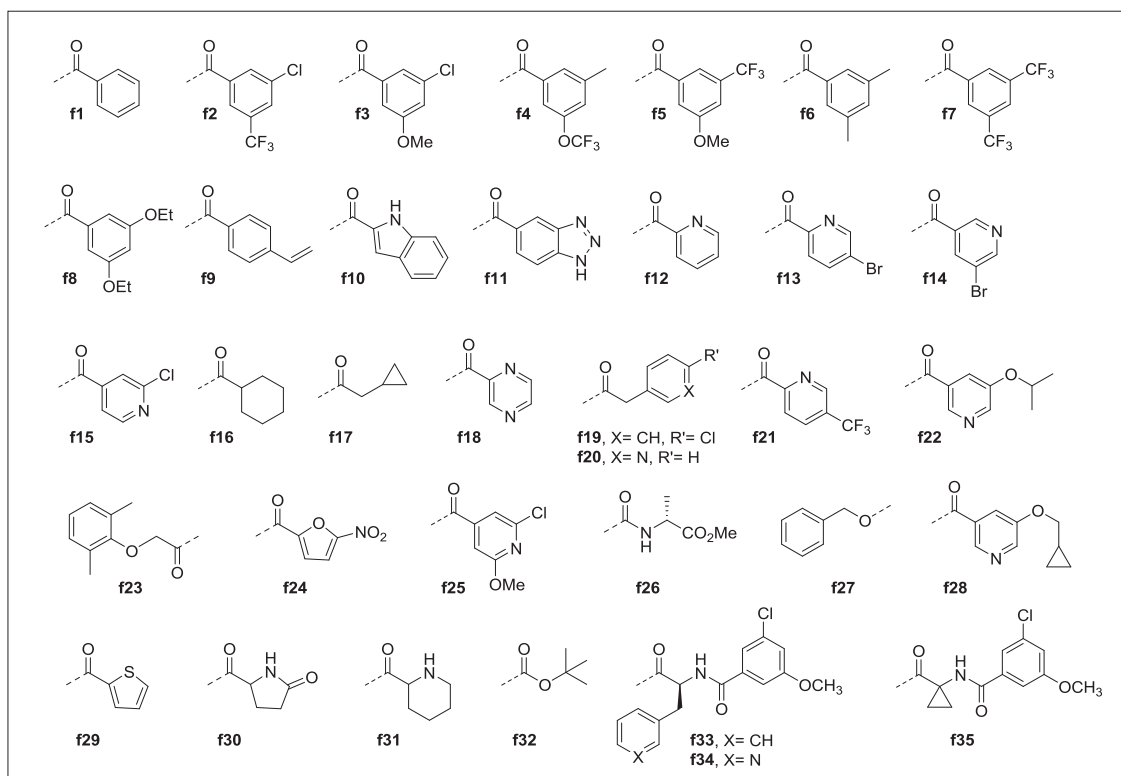
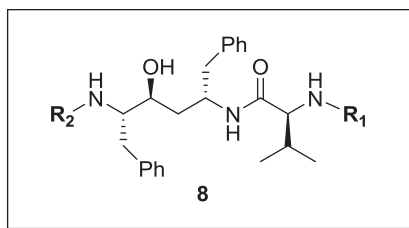


**Figure 4.** Structures of fragments f1 to f35 used for the synthesis of the compound library with general structure 8 (Fig. 5).

hydroxyethylene moiety of compounds such as 4, 5 and 6, whereas, inhibitors of zinc metalloproteases often have a phosphinic acid pharmacophore, which serves as a bioisostere of the metal chelating

transition state (Fig. 3).<sup>24</sup> Interestingly, HIV PIs that have been reported to inhibit ZMPSTE24 (*i.e.* 4–6) are characterized by aromatic moieties at both the P1 and the P1' residues (*i.e.* binding to the S1 and S1'



<b>8a</b> , R <sub>1</sub> = f23, R <sub>2</sub> = f23	<b>8n</b> , R <sub>1</sub> = f30, R <sub>2</sub> = f23
<b>8b</b> , R <sub>1</sub> = f2, R <sub>2</sub> = f23	<b>8o</b> , R <sub>1</sub> = f6, R <sub>2</sub> = f21
<b>8c</b> , R <sub>1</sub> = f3, R <sub>2</sub> = f23	<b>8p</b> , R <sub>1</sub> = f25, R <sub>2</sub> = f23
<b>8d</b> , R <sub>1</sub> = f4, R <sub>2</sub> = f23	<b>8q</b> , R <sub>1</sub> = f33, R <sub>2</sub> = f23
<b>8e</b> , R <sub>1</sub> = f5, R <sub>2</sub> = f23	<b>8r</b> , R <sub>1</sub> = f34, R <sub>2</sub> = f23
<b>8f</b> , R <sub>1</sub> = f6, R <sub>2</sub> = f23	<b>8s</b> , R <sub>1</sub> = f12, R <sub>2</sub> = f23
<b>8g</b> , R <sub>1</sub> = f7, R <sub>2</sub> = f23	<b>8t</b> , R <sub>1</sub> = f24, R <sub>2</sub> = f23
<b>8h</b> , R <sub>1</sub> = f8, R <sub>2</sub> = f23	<b>8u</b> , R <sub>1</sub> = f13, R <sub>2</sub> = f23
<b>8i</b> , R <sub>1</sub> = f9, R <sub>2</sub> = f23	<b>8v</b> , R <sub>1</sub> = f11, R <sub>2</sub> = f23
<b>8j</b> , R <sub>1</sub> = f19, R <sub>2</sub> = f23	<b>8w</b> , R <sub>1</sub> = f16, R <sub>2</sub> = f23
<b>8k</b> , R <sub>1</sub> = f20, R <sub>2</sub> = f23	<b>8x</b> , R <sub>1</sub> = f31, R <sub>2</sub> = f23
<b>8l</b> , R <sub>1</sub> = f15, R <sub>2</sub> = f23	<b>8y</b> , R <sub>1</sub> = f17, R <sub>2</sub> = f23
<b>8m</b> , R <sub>1</sub> = f21, R <sub>2</sub> = f23	

**Figure 5.** Select examples of compounds designed to explore prelamins A accumulation, plausibly by inhibiting ZMPSTE24. The exact structures of all the fragments used for this library (*i.e.* f1 to f35) are shown in Fig. 4.

pocket; Fig. 3), whereas the structurally related compound darunavir, having an isopropyl group at P1' was reported to not inhibit ZMPSTE24.<sup>25</sup> Additionally, a number of phosphinic acid-based inhibitors of therapeutically important zinc metalloproteases are also characterized by P1 and P1' aryl substituents; examples include analog **7a**, a dual inhibitor of the endothelin converting enzyme (ECE) and neutral endopeptidase (NEP)<sup>26</sup> and **7b**, a dual inhibitor of angiotensin converting enzyme (ACE) C-domain and the endothelin converting enzyme-1 (ECE-1).<sup>27</sup> Accordingly, the minimal consensus scaffold represented by the general structures **8** and **13** (Fig. 3) was designed and the synthesis of a 65-member library was initiated in search of hits binding to ZMPSTE24. The building blocks shown in Fig. 4 were selected as the diversity elements at substituents -R<sub>1</sub> and -R<sub>2</sub>; select examples from this library of compounds are shown in Fig. 5.

### 2.1. Synthesis of peptidomimetic analogs **8**

Enantioselective synthesis of the hydroxyethylene dipeptide bioisostere **11** was previously reported (Scheme 1).<sup>28</sup> In brief, the formation of enantiomerically enriched intermediate **11** was dictated by the chirality of L-phenylalanine and intramolecular hydrogen bonding between the -NH<sub>2</sub> group and the ketone of the enaminone **10**, leading to the formation of an ~18:1 diastereomeric ratio of ketones (after the first reduction step).<sup>28</sup> Additionally, the presence of the two bulky protecting groups on the α-amine of phenylalanine is assumed to bias the reduction of the ketone **10** to the desired β-alcohol in high enantiomeric purity (*i.e.* in the second reduction step).<sup>29</sup> For the preparation of our library, the doubly reduced product **11** (desired diastereomer isolated in 55% yield) was condensed with S-4-isopropylloxazolidine-2,5-dione (prepared as previously reported<sup>30</sup>) and the free amine of the valine moiety was Boc-protected. After debenzoylation of the phenylalanine to obtain intermediate **12**, various -R<sub>2</sub> moieties were introduced, usually from an acid chloride, such as the 2-

(2,6-dimethylphenoxy)acetyl group found in lopinavir (*i.e.* fragment f23). Subsequently, deprotection of the N-Boc group of the valine moiety under standard TFA conditions and coupling of various carboxylic acids, using standard peptide coupling chemistry, introduced various -R<sub>1</sub> groups to give analogs **8** (Scheme 1); specific examples from this library are shown in Figure 5.

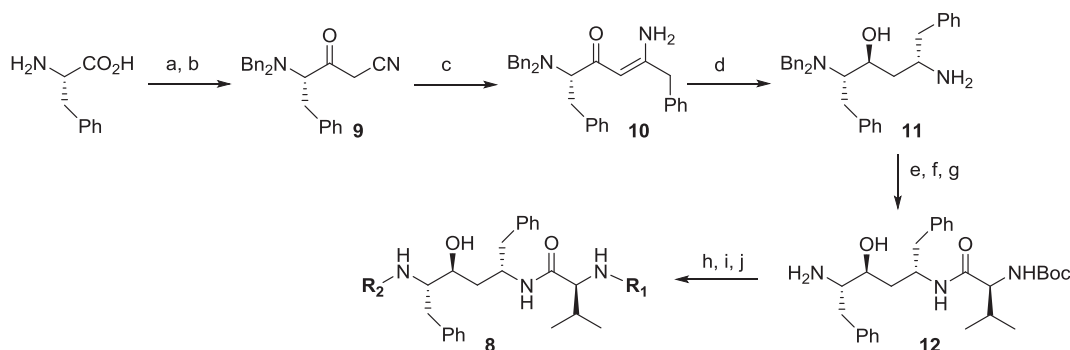
### 2.2. Synthesis of phosphinic acid-based analogs **13**

In spite of the significant similarities, in both structure and function, between the bacterial zinc metalloprotease thermolysin (TLN) and ZMPSTE24, neither inhibitors of TLN nor inhibitors of any other zinc metalloprotease have been reported to inhibit ZMPSTE24 or block prelamins A accumulation in cells. Interestingly, TLN was used to model a tetrapeptide ligand bound to the human ZPMSTE24 and the resemblance between the active sites of ZMPSTE24 and TLN was highlighted.<sup>2</sup> We decided to probe the ability of phosphinyl peptides to block prelamins A processing and consequently, we synthesized derivatives **13**, based again on the minimal consensus model shown in Fig. 3. In a previous study, screening of hydrophobic amino acids at the C-terminal of tripeptide ligands (*i.e.* residue presumed to bind in the S<sub>2</sub>' sub-pocket of the active site) identified alanine as the residue providing the most potent phosphonamidic acid inhibitors of TLN (*e.g.* compound **14**, Fig. 6).<sup>31</sup> We decided to incorporate this finding in the design of our phosphinic acid-based analogs **13**, as well as maintained the Cα and Cβ' benzyl substituents, which presumably could bind in the S1 and S1' sub-pockets of the active site (Fig. 3).

Synthesis of compounds **13a,b** was initiated with the three-component condensation of diphenylmethanamine hydrochloride, phenyl acetaldehyde and hypophosphorous acid to give N-protected phosphinic acid **15**, as previously reported (Scheme 2).<sup>32</sup> Deprotection of the amine moiety under acidic conditions, followed by coupling with benzyl chloroformate produced the racemic Cbz-protected aminophosphinic acid **16**, which was subsequently converted to its diastereomeric salt with R-(+)-methylbenzylamine. The desired R-enantiomer of **16** was isolated after two recrystallizations in moderate yield; all characterization data were consistent with those previously reported, including the high optical purity, which was based on the reported optical rotation.<sup>32</sup> Intermediate R-**16** was condensed with the acrylate **17**; the latter reagent was prepared in two steps from diethyl 2-benzylmalonate, which was converted to the acrylate via a Mannich-type reaction and simultaneous *in situ* decarboxylation.<sup>33</sup> The trivalent phosphorus species, generated by heating **16** with neat hexamethyldisilazane (HMDS), condensed with **17** via a phospho-Michael addition to give the phosphinate **18** in good yield. The <sup>31</sup>P NMR of **18** indicated that a single set of diastereomers was formed, confirming the high enantiomeric purity of R-**16**. However, for the purpose of this study, authentic standards were not synthesized and consequently, the exact %ee was not determined. After saponification of **18** and coupling with the methyl ester of L-alanine under standard peptide coupling conditions, the methyl ester **13a** was obtained, which was first purified by C-18 reversed phase HPLC and then saponified to give the free C-terminal carboxylic acid **13b** (Scheme 2).

### 2.3. Biological evaluation of key analogs from general structure **8** and **13**

In spite of several previous efforts,<sup>18,20a,23</sup> the development of a high-throughput and reliable *in vitro* assay for measuring the catalytic turnover of ZMPSTE24 remains a significant challenge. Highly membrane-bound enzymes are typically rendered soluble in buffer by either cleaving a "tail" peptide that anchors them into a membrane (*i.e.* creating a catalytically relevant mutant) or by suspending them in high concentrations of protein-detergents complexes or micelle preparations; in the case of ZMPSTE24 only the latter approach is feasible. However, this approach often leads to artifacts that can derail SAR studies in medicinal chemistry. Previously, detecting ligand binding to ZMPSTE24



**Scheme 1.** Synthesis of a compound library with general structure **8**; fragments f1–f35 were used for  $R_1$  and  $R_2$  (Fig. 5). Reagents and conditions: (a) BnBr,  $K_2CO_3$ ,  $H_2O$ , reflux, 24 h, 88%; (b)  $CH_3CN$ ,  $NaNH_2$ , THF, Ar,  $-45^\circ C$ , 82%; (c) i. BnMgBr, THF,  $0^\circ C$  to RT, ii. 10% aqueous citric acid quench, 92%; (d) i.  $NaBH_4$ , MsOH, THF/*i*PrOH,  $10^\circ C$ , ii.  $NaBH_4$ , TFA,  $10^\circ C$ , 55%; (e) *S*-4-isopropylloxazolidine-2,5-dione,  $Et_3N$ ,  $CH_2Cl_2$ , Ar,  $-15^\circ C$ , 97%; (f)  $(BOC)_2O$ ,  $Et_3N$ ,  $CH_2Cl_2$ ,  $0^\circ C$  to RT, 90%; (g)  $H_2$  (1 atm),  $Pd(OH)_2/C$ , MeOH, RT, 80%; (h)  $R_2COCl$ ,  $NaHCO_3$ ,  $EtOAc:H_2O$ , Ar, RT, 75–85%; (i) TFA,  $CH_2Cl_2$ , RT, 70–75%; (j)  $R_1CO_2H$ , HBTU, DIPEA, DMF, Ar, RT, 50–90%.

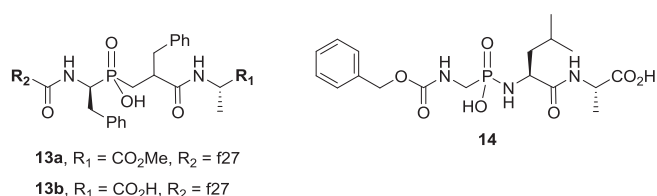
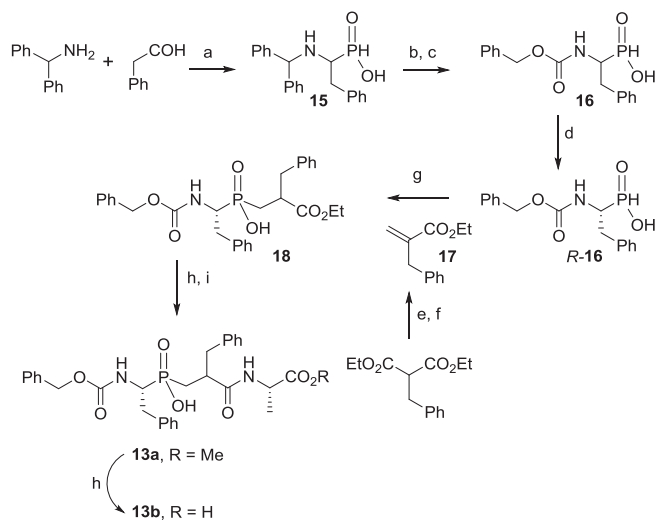


**Figure 6.** Structures of phosphinic acid-based analogs **13**; the shared consensus scaffold with the hydroxyethylene analogs **8** is highlighted (the structure of fragment f27 is shown in Fig. 5).



**Scheme 2.** Synthesis of phosphinic acid analogs **13**. Reagents and conditions: (a)  $H_3PO_2$ ,  $EtOH:H_2O$ ,  $90^\circ C$ , 5.5 h, 76%; (b) 48% aq. HBr, propylene oxide,  $100^\circ C$ , 2.5 h, 90%; (c)  $CbzCl$ ,  $NaOH$ ,  $H_2O$ ,  $0^\circ C$  to RT, 5 h, 91%; (d) *R*-(+)-methylbenzylamine,  $EtOH$ ,  $HCl$ , 41%; (e)  $KOH$ ,  $EtOH$ , RT, 24 h; (f)  $Et_3NH$ , 37% aq.  $CH_2O$ ;  $0^\circ C$  to RT, 7 h, 68% over last two steps; (g) HMDS,  $110^\circ C$ , 2 h, 73%; (h)  $NaOH$ ,  $EtOH$ ,  $H_2O$ ,  $0^\circ C$  to RT, 48 h, 84%; (i) alanine methylester hydrochloride, EDC, HOBT, DIPEA,  $CH_2Cl_2$ , RT, 2.5 h, 84%.

relied on high-resolution mass spectrometry of the protein-inhibitor complex,<sup>34</sup> or indirect *in vitro* inhibition assays that were coupled to the methylation step catalyzed by ICMT (i.e. detecting  $^{14}C$ -incorporation from *S*-adenosyl-L-[methyl- $^{14}C$ ]methionine).<sup>23,35</sup>

We decided to initiate efforts towards the discovery of novel hits targeting ZMPSTE24 using a phenotypic, cell-based assay that measures the accumulation of farnesylated prelamin A in cells treated with a compound. Although cell-based assays do not usually support the development of a reliable SAR model, they have the advantage of

providing hits with better drug-like properties (e.g. cell membrane permeability). Based on the minimal consensus scaffold of analogs **8** and **13**, designed to resemble the key structural motifs binding to the S1 and S1' sub-pockets of known aspartic protease<sup>36</sup> and zinc metalloproteases, a 65-member library was synthesized. All members of this library were initially screened at a fixed concentration of  $10\ \mu M$  in human osteosarcoma cells (U-2 OS) for their ability to induce prelamin A accumulation. U-2 OS cells were incubated with each compound for 24 h and then their cell lysates were analyzed by Western Blots using a prelamin A-specific antibody; the results from select compounds are shown in Fig. 7. The levels of prelamin A were compared to tubulin,

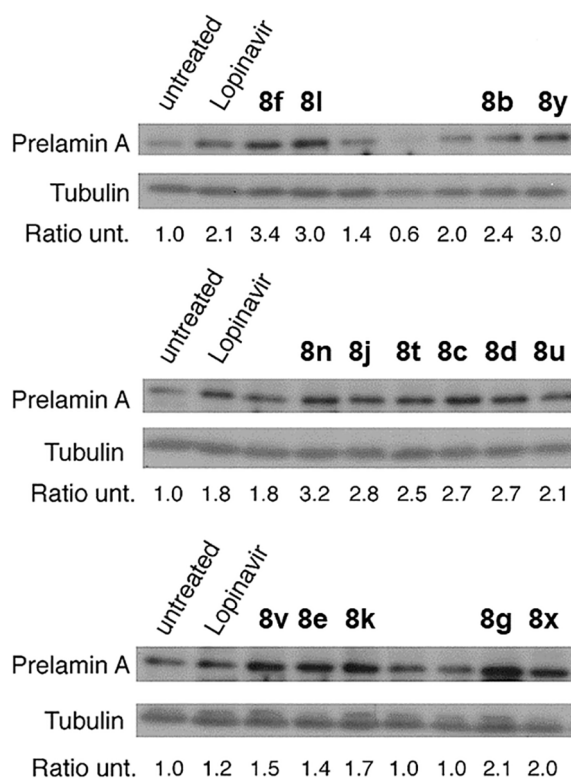
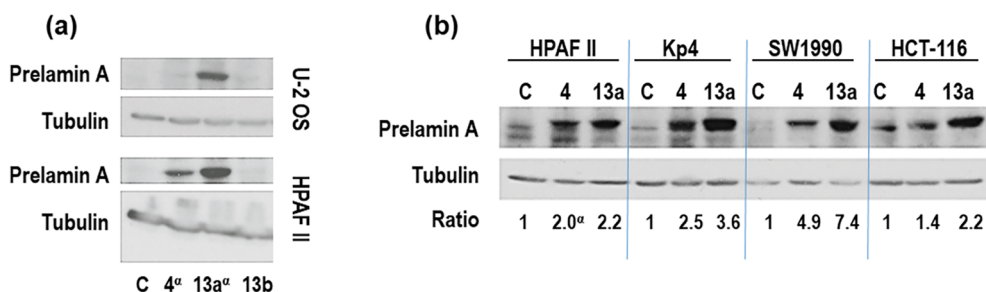


**Figure 7.** Western Blot analysis of intracellular accumulation of prelamin A in human osteosarcoma cells (U-2 OS); ratio units represent prelamin A levels vs. levels of tubulin in treated cells as compared to the control (the ratio of prelamin A levels to tubulin was arbitrarily set to 1 for the untreated control cells); lopinavir was tested in parallel as a reference and only compounds that induced a higher level of intracellular prelamin A accumulation than lopinavir are specifically indicated.



ratios were difficult to estimate.

since tubulin expression should not be altered by biochemical events associated with the biosynthesis or processing of prelamin A. To adjust for the normal variability between assays, lopinavir (4) was tested in parallel as the reference control. Several analogs were identified that induced greater accumulation of prelamin A than lopinavir (*albeit* only modestly greater), including compounds **8f**, **8k**, **8l**, **8n**, **8g** (Fig. 7), as well as the phosphinyl analog **13a** (Fig. 8a). Interestingly, the carboxylic acid analog **13b** was inactive at the concentration tested (10  $\mu$ M), possibly due to lower cell permeability than its corresponding methyl ester **13a** (Fig. 8a). Compound **13b** was previously explored as an inhibitor of the neutral endopeptidase (NEP)<sup>26</sup> and the endothelin converting enzyme (ECE),<sup>26</sup> as well as a dual inhibitor of neprilysin (neutral endopeptidase) and aminopeptidase N that are associated with the degradation of enkephalins.<sup>37</sup> Additionally, **13b** was also previously explored as a potential angiotensin converting enzyme 2 inhibitor, but found to be essentially inactive ( $K_i > 10 \mu$ M).<sup>38</sup>

According to microarray studies available in Oncomine, ZMPSTE24 is overexpressed in many human cancers, including glioma, melanoma, ovarian, prostate and pancreatic cancers. To further probe the effects of our compounds, we tested one of our best analogs, compound **13a**, in pancreatic adenocarcinoma cells (HPAF II, SW1990 and KP-4), and human colon cancer cells (HCT-116). In general, higher intracellular accumulation of the farnesylated prelamin A was observed with **13a** as

compared to lopinavir in all cases (Fig. 8).

Further biological evaluation of compound **13a** in our most highly tumorigenic pancreatic cancer cell lines (HPAF-II and KP-4) revealed that despite accumulation of prelamin A, proliferation was not significantly affected in these cells (Fig. 9a). Consistent with this observation, treatment of HPAF-II and KP-4 cells with **13a** did not lead to accumulation of the proliferation inhibitor p21 nor reduction in the expression levels of the proliferation biomarker MCM6 (Fig. 9b). However, in a transmigration potential assay,<sup>39</sup> analog **13a** was found to inhibit cell migration, whereas lopinavir (4) did not have any apparent effect (Fig. 9c). Metastasis remains a leading cause of mortality from cancer. Cancer cell migration through connective tissues requires that cells undergo large distortions in order to crawl through constricted spaces of tissue matrix. It has been shown that intracellular levels of lamin A modulate the elasticity/stiffness of solid tumors and consequently, the nuclear plasticity of cancer cells plays a key role in the 3D migration of these cells.<sup>39,40</sup> Even a very modest increase in intracellular prelamin A levels (10%) has been reported to inhibit the migration of lung cancer cells A549 by 90%.<sup>41</sup> These findings suggest that although modest increase in intracellular levels of prelamin A accumulation may not lead to any cell toxicity, it may still have therapeutic value in deterring cancer metastasis. Therefore, optimization of compounds such as **8f** and **13a** is worth pursuing as potential

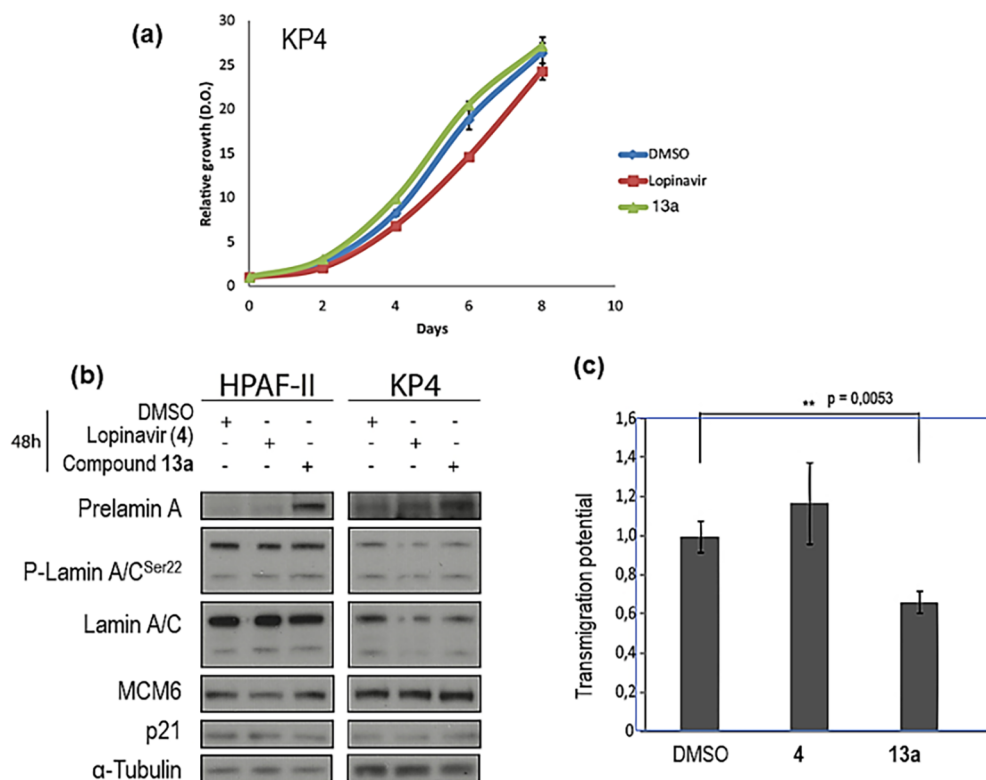


**Figure 9.** Biological profiling of analog **13a** in human pancreatic adenocarcinoma cells (HPAF II and KP-4). (a) Cell proliferation assay data using KP-4 cells. (b) Western Blot analysis of proteins levels, including prelamin A; (c) Transmigration assay in KP-4 cells; lopinavir (4) and 0.15% DMSO (vehicle) in buffer were used as controls. Compounds **4** and **13a** were tested at a single concentration of 10  $\mu$ M.

therapeutics in oncology.

### 3. Conclusion

Lamins are an integral part of the nuclear envelope proteins and play a critical role in nuclear stability, as well as in numerous other biochemical processes that are incompletely understood at this time. Recent studies have shown that accumulation of high levels of the farnesylated prelamin A protein around the nuclear membrane induces abnormalities to the nuclear shape, resulting in polyploid cells and exhibiting features of cellular senescence that trigger an antitumor response.<sup>42</sup> The nucleoskeletal properties of farnesylated prelamin A confer cell stiffness and downregulate cancer cell migration/metastasis. This precursor protein must undergo four post-translational modifications, including two proteolytic steps catalyzed by the zinc metalloprotease STE24 (ZPMSTE24), to produce the mature lamin A. A number of recent biochemical studies suggest that inhibition of ZPMSTE24 leads to prelamin A accumulation at the nuclear envelope, thus compromising cell division, impairing mitosis and inducing cell senescence. The biochemical consequences of ZPMSTE24 inhibition suggest that this enzyme may be a valuable therapeutic target for both the treatment of cancer and the prevention of metastasis.

Although the development of an *in vitro* assay that is reliable for guiding medicinal chemistry efforts remains a challenge for this enzyme, phenotypic drug discovery can be an alternative approach, which can provide hits with better initial drug-like properties (e.g. cell membrane permeability). Phenotypic screening is a complimentary approach to the more traditional target-based screening with the potential to allow interrogation of yet incompletely understood biochemical processes that are associated with a disease.<sup>43</sup> A library of compounds was synthesized based on the consensus tripeptide-like core of known aspartate protease and zinc metalloprotease inhibitors. All analogs were screened using Western Blot analysis of prelamin A accumulation in cancer cells and compared to lopinavir, a previously reported inhibitor of ZPMSTE24.<sup>20,23,25,34</sup> Several analogs were identified with sufficient cell permeability to induce intracellular accumulation of prelamin A in osteosarcoma (U-2 OS), pancreatic adenocarcinoma (HPAFII, SW1990, KP-4) and colon carcinoma (HCT-116) cells. Some of these compounds were more potent than lopinavir in blocking prelamin A processing, without exhibiting any overt toxicity to cells. However, even when the level of toxicity was nearly negligible, as in the case of the highly tumorigenic pancreatic cancer cells KP-4, treatment of these cells with the most potent analog **13a** led to simultaneous accumulation of prelamin A and inhibition in cell migration. Cell migration requires the deformation of the nucleus, as previously demonstrated in neutrophils that possess a multi-lobulated nucleus and express low levels of mature lamin A.<sup>44</sup> Furthermore, cell migration is a necessary biological event for tumor cell dissemination and consequently, our data suggests that analog **13a** represents a valuable hit for optimization into inhibitors of prelamin A processing, which even at sub-toxic concentration can have anti-metastatic effect.<sup>45</sup> Potency optimization and target engagement studies that will confirm binding of our inhibitors to ZPMSTE24 in cells are currently in progress.

### Acknowledgments

Financial support for this work was provided from research grants from the Canadian Institute of Health Research (CIHR) and the Natural Sciences and Engineering Research Council of Canada (NSERC) to G. Ferbeyre and Y.S. Tsantrizos, respectively.

### Appendix A. Supplementary data

Supplementary data to this article can be found online at <https://doi.org/10.1016/j.bmc.2018.10.001>.

### References

- (a) Young SG, Fong LG, Michaelis S. Prelamin A, Zmpste24, misshapen cell nuclei, and Progeria - new evidence suggesting that protein farnesylation could be important for disease pathogenesis. *J. Lipid Res.* 2005;46:2531–2558;
  - Barrowman J, Michaelis S. ZMPSTE24, an integral membrane zinc metalloprotease with a connection to progeroid disorders. *Biol Chem.* 2009;390:761–773.
- Quigley A, Dong YT, Pike AC, et al. The structural basis of ZMPSTE24-dependent laminopathies. *Science.* 2013;339:1604–1607.
- Schmitt CA. Senescence, apoptosis and therapy – Cutting the lifelines of cancer. *Nat Rev Cancer.* 2003;3:286–294.
- (a) Xue W, Zender L, Miething C, et al. Senescence and tumour clearance is triggered by p53 restoration in murine liver carcinomas. *Nature.* 2007;445:656–660;
  - Kang TW, Yevsa T, Woller N, et al. Senescence surveillance of pre-malignant hepatocytes limits liver cancer development. *Nature.* 2011;479:547–551.
- (a) De Sandre-Giovannoli A, Bernard R, Cau P, Navarro C, Amiel J, Buccaccio I, Lyonnet S, Stewart CL, Munnich A, Le Merrer M, Lévy N. Lamin A truncation in Hutchinson-Gilford progeria. *Science.* 2003;300:2055;
  - Eriksson M, Brown WT, Gordon LB, et al. Recurrent de novo point mutations in lamin A cause Hutchinson-Gilford progeria syndrome. *Nature.* 2003;423:293–298;
    - Hennekam RCM. Hutchinson-Gilford progeria syndrome: review of the phenotype. *Am J Med Genet A.* 2006;140:2603–2624.
- Liu B, Wang J, Chan KM, et al. Z. Genomic instability in laminopathy-based premature aging. *Nat Med.* 2005;11:780–785.
- Benson EK, Lee SW, Aaronson SA. Role of progerin-induced telomere dysfunction in HGPS premature cellular senescence. *J Cell Sci.* 2010;123:2605–2612.
- (a) Krishnan V, Chow MZY, Wang Z, et al. Histone H4 lysine 16 hypoacetylation is associated with defective DNA repair and premature senescence in Zmpste24-deficient mice. *Proc Natl Acad Sci USA.* 2011;108:12325–12330;
  - Shumaker DK, Dechat T, Kohlmaier A, et al. Mutant nuclear lamin A leads to progressive alterations of epigenetic control in premature aging. *Proc Natl Acad Sci USA.* 2006;103:8703–8708.
- Cao K, Capell BC, Erdos MR, Djabali K, Collins FS. A lamin A protein isoform overexpressed in Hutchinson-Gilford progeria syndrome interferes with mitosis in progeria and normal cells. *Proc Natl Acad Sci USA.* 2007;104:4949–4954.
- Goldman RD, Shumaker DK, Erdos MR, et al. F.S. Accumulation of mutant lamin A causes progressive changes in nuclear architecture in Hutchinson-Gilford progeria syndrome. *Proc Natl Acad Sci USA.* 2004;101:8963–8968.
- Varela I, Pereira S, Ugalde AP, et al. Combined treatment with statins and aminobisphosphonates extends longevity in a mouse model of human premature aging. *Nat Med.* 2008;14:767–772.
- Gordon LB, Kleinman ME, Miller DT, et al. Clinical trial of a farnesyltransferase inhibitor in children with Hutchinson - Gilford progeria syndrome. *Proc Natl Acad Sci USA.* 2012;109:1666–16671.
- Gordon LB, Kleinman ME, Massaro J, et al. Clinical Trial of the Protein Farnesylation Inhibitors Lonafarnib, Pravastatin, and Zoledronic Acid in Children With Hutchinson-Gilford Progeria Syndrome. *Circulation.* 2016;134:114–125.
- Shalev SA, De Sandre-Giovannoli A, Shani AA, Levy N. An association of Hutchinson-Gilford progeria and malignancy. *Am J Med Genet A.* 2007;143A:1821–1826.
- de la Rosa J, Freije JMP, Cabanillas R, Osorio FG, Fraga MF, Soledad Fernández-García MS, Rad R, Fanjul V, Ugalde AP, Liang Q, Prosser HM, Bradley A, Cadimanos J, López-Otín C. Prelamin A causes progeria through cell-extrinsic mechanisms and prevents cancer invasion. *Nat Commun.* 2013;4:2268. <https://doi.org/10.1038/ncomms3268>.
- Lacbay CM, Waller DD, Park J, Gómez Palou M, Vincent F, Huang XF, Ta V, Berghuis AM, Sebarg M, Tsantrizos YS. Unraveling the Prenylation-Cancer Paradox in Multiple Myeloma with Novel GGPPS Inhibitors. *J. Med. Chem.* 2018 ASAP.
- Pellejeux S, Picard C, Lamarre-Théroux L, et al. Isoprenoids and tau pathology in sporadic Alzheimer's disease. *Neurobiol Aging.* 2018;65:132–139.
- Clark KM, Jenkins JL, Fedoriv N, Dumont ME. Human CaaX protease ZMPSTE24 expressed in yeast: Structure and inhibition by HIV protease inhibitors. *Protein Sci.* 2017;26:242–257.
- Pryor Jr EE, Horanyi PS, Clark KM, et al. Structure of the integral membrane protein CAAx protease Ste24p. *Science.* 2013;339:1600–1604.
- (a) Coffinier C, Hudon SE, Farber EA, et al. HIV protease inhibitors block the zinc metalloproteinase ZMPSTE24 and lead to an accumulation of prelamin A in cells. *Proc Natl Acad Sci USA.* 2007;104:13432–13437;
  - Clarke SG. HIV protease inhibits and nuclear lamin processing: Getting the right bells and whistles. *Proc Natl Acad Sci USA.* 2007;104:13857–13858.
- Bonello-Palot N, Simoncini S, Robert S, et al. Prelamin A accumulation in endothelial cells induces premature senescence and functional impairment. *Atherosclerosis.* 2014;237:45–52.
- Perrin S, Cremer J, Faucher O, Reynes J, Dellamonica P, Micallef J, Solas C, Lacarelle B, Stretti C, Kaspi E, Robaglia-Schlupp A, Tamalet CN-BC, Lévy N, Poizat-Martin I, Cau P, Patrice Roll P. HIV protease inhibitors do not cause the accumulation of prelamin A in PBMCs from patients receiving first line therapy: the ANRS EP45 “Aging” study. *PLoS ONE.* 2012;7(12):e33035.
- Chang SY, Hudon-Miller S, Yang SH, et al. Inhibitors of protein geranylgeranyl transferase-I lead to prelamin A accumulation in cells by inhibiting ZMPSTE24. *J*

- Lipid Res.* 2012;53:1176–1182.
24. (a) Bohacek R, De Lombaert S, McMartin C, Priestle J, Grütter M. Three-Dimensional Models of ACE and NEP Inhibitors and Their Use in the Design of Potent Dual ACE/NEP Inhibitors. *J Am Chem Soc.* 1996;118:8231–8249;
- (b) Cramer J, Krimmer SG, Fridh V, et al. Elucidating the origin of long residence time binding for inhibitors of the metalloprotease thermolysin. *ACS Chem Bio.* 2017;12:225–233.
25. Coffinier C, Hudon SE, Lee R, et al. A potent HIV protease inhibitor, Darunavir, does not inhibit ZMPSTE24 or lead to an accumulation of farnesyl-prelamin A in cells. *J Biol Chem.* 2008;283:9797–9804.
26. Lloyd J, Schmidt JB, Hunt JT, Barrish JC, Little DK, Tymiak AA. Solid phase synthesis of phosphonic acid endothelin converting enzyme inhibitors. *Bioorg Med Chem Lett.* 1996;6:1323–1326.
27. Jullien N, Makritis A, Georgiadis D, Beau F, Yiotakis A, Dive V. Phosphinic tripeptides as dual angiotensin-converting enzyme C-domain and endothelin-converting enzyme-1 inhibitors. *J Med Chem.* 2010;53:208–220.
28. Stuk TL, Haight AR, Scarpetti D, et al. An efficient stereocontrolled strategy for the synthesis of hydroxyethylene dipeptide isosteres. *J Org Chem.* 1994;59:4040–4041.
29. For a review refer to: Tramontini, M. *Synthesis* 1982, pp. 605–644.
30. Daly WH, Poche D. The preparation of *N*-Carboxyanhydrides of  $\alpha$ -amino acids using bis(trichloromethyl)carbonate. *Tetrahedron Lett.* 1988;29:5859–5862.
31. Biela A, Nasief NN, Betz M, Heine A, Hangauer D, Klebe G. Dissecting the hydrophobic effect on the molecular level: the role of water, enthalpy and entropy in ligand binding to thermolysin. *Angew Chem Int Ed.* 2013;52:1822–1828.
32. Baylis EK, Campbell CD, Dingwall JG. 1-Aminoalkylphosphonous acids. Part 1. Isosteres of the protein amino acids. *J Chem Soc Perkin Trans.* 1984;1:2845–2853.
33. (a) Liu X, Hu E, Tian X, Mazur A, Ebetino FH. Enantioselective synthesis of phosphinyl peptidomimetics via an asymmetric Michael reaction of phosphinic acids with acrylate derivatives. *J Organometal Chem.* 2002;646:212–222;
- (b) Matziari M, Bauer K, Dive V, Yiotakis A. Synthesis of the phosphinic analogue of thyrotrophin releasing hormone. *J Org Chem.* 2008;73:8591–8593.
34. Mehmood S, Marcoux J, Gault J, et al. Mass spectrometry captures off-target drug binding and provides mechanistic insight into the human metalloprotease ZMPSTE24. *Nat Chem.* 2016;8:1152–1158.
35. (a) Corrigan DP, Kuszczak D, Rusinol AE, et al. Prelamin A endoproteolytic processing *in vitro* by recombinant Zmpste24. *Biochem J.* 2005;387:129–138.
36. Tsantrizos YS. Peptidomimetic therapeutic agents targeting the protease enzyme of the human immunodeficiency virus and hepatitis C virus. *Acc Chem Res.* 2008;41:1252–1263.
37. Chen H, Noble F, Mothé A, et al. Phosphinic derivatives as new dual encephalin-degrading enzyme inhibitors: Synthesis, biological properties, and antinociceptive activities. *J Med Chem.* 2000;43:1398–1408.
38. Mores A, Matziari M, Beau F, Cuniasso P, Yiotakis A, Dive V. Development of potent and selective phosphinic peptide inhibitors of angiotensin-converting enzyme 2. *J Med Chem.* 2008;51:2216–2226.
39. Wolf K, te Lindert M, Krause M, et al. Physical limits of cell migration: Control by ECM space and nuclear deformation and tuning by proteolysis and traction force. *J Cell Biol.* 2013;201:1069–1084.
40. Swift J, Ivanovska IL, Buxboim A, et al. Nuclear lamin-A scales with tissue stiffness and enhances matrix-directed differentiation. *Science.* 2013;341:1240104. <https://doi.org/10.1126/science.1240104>.
41. Harada T, Swift J, Irianto J, et al. Nuclear lamin stiffness is a barrier to 3D migration, but softness can limit survival. *J Cell Biol.* 2014;204:669–682.
42. Moiseeva O, Lessard F, Acevedo-Aquino M, Tsantrizos Vernier M, Y.S., Ferbeyre, G.. Mutant lamin A links prophase to a p53 independent senescence program. *Cell Cycle.* 2015;14:2408–2421.
43. For a recent review see: Moffat JG, Vincent F, Lee JA, Eder J, Prunotto M. Opportunities and challenges in phenotypic drug discovery: an industry perspective. *Nat Rev Drug Discov.* 2017;16:531–543.
44. Shin J-W, Spinler KR, Swift J, Chasis JA, Mohandas N, Discher DE. Lamins regulate cell trafficking and lineage maturation of adult human hematopoietic cells. *Proc Natl Acad Sci USA.* 2013;110:18892–18897.
45. For a recent review see: Davidson PM, Lammerding J. Broken nuclei - lamins, nuclear mechanics, and disease. *Trends Cell Biol.* 2014;24:247–256.